

Deep Inelastic Atomic Scattering of X Rays in Liquid Neon

G. Monaco,¹ A. Cunsolo,² G. Pratesi,³ F. Sette,¹ and R. Verbeni¹

¹European Synchrotron Radiation Facility, Boîte Postale 220 F-38042 Grenoble Cedex 9, France

²Dipartimento di Fisica and Istituto Nazionale di Fisica della Materia, Università di Roma Tre, I-00146 Roma, Italy

³Dipartimento di Fisica and Istituto Nazionale di Fisica della Materia, Università di Firenze, I-50125 Firenze, Italy

(Received 19 November 2001; published 15 May 2002)

An inelastic x-ray scattering (IXS) experiment in liquid neon has been performed in the ± 100 meV exchanged energy range and at exchanged wave numbers, q , comprised between 1 and 16 \AA^{-1} . At the highest probed q 's a deep inelastic scattering regime is reached where the Ne core electrons, after collision with the x rays, recoil almost freely with an effective mass equal to the Ne atomic mass. IXS in this high q regime is here shown to provide quantitative information on the atomic momentum distribution of liquid Ne, thus supplying a complementary technique to neutron scattering. There are several open problems in quantum and classical liquids which can benefit from this complementarity.

DOI: 10.1103/PhysRevLett.88.227401

PACS numbers: 78.70.Ck, 61.10.Eq, 61.25.Bi

Deep inelastic scattering experiments are used in many research areas of physics as a tool to determine the momentum distribution in the probed system [1]. The basic idea of these experiments is quite simple. If the energy and the momentum which are transferred in the scattering event from the probe particle to the target particle are very high compared to the characteristic energy and momentum of the target particle, the latter can be considered to recoil freely from the collision, and the scattered probe particle carries information on the initial momentum distribution of the target particle.

If one chooses x rays as a probe, their interaction with the target occurs, in a weakly relativistic limit, via the electromagnetic coupling with the electrons of the target system. At high exchanged energies the spectrum of the scattered x rays reflects the electronic excitations, and this is the part of the spectrum which is traditionally studied in inelastic x-ray scattering (IXS) experiments [2]. In this case, the deep inelastic scattering regime is the Compton limit [3]; there, it is an electron momentum distribution that is experimentally accessed to. Conversely, the low energy part of the spectrum of the scattered x rays reflects, via the adiabatic approximation, the atomic dynamics [2]. In fact, the nonresonant IXS cross section per unit exchanged energy, E , and unit solid angle, Ω , for the simple case of a monatomic target system and in the small exchanged energies limit can be approximated as [2]

$$\frac{\partial^2 \sigma}{\partial E \partial \Omega} = r_0^2 |\epsilon_i \cdot \epsilon_f|^2 \frac{k_f}{k_i} |f(q)|^2 S(q, E). \quad (1)$$

Here r_0 is the classical electron radius; ϵ_α and \mathbf{k}_α are the polarization and the wave vector of the incident (subscript i) and scattered (subscript f) x rays; q is the wave vector exchanged by the incident photons in the scattering process; $f(q)$ is the atomic form factor; $S(q, E)$ is the dynamic structure factor, and contains the relevant atomic dynamics information.

In this Letter, we show that it is possible to select an appropriate energy and momentum transfer range where the

scattering of x rays can be used to obtain quantitative information, via the dynamic structure factor, on the atomic momentum distribution, thus providing a complementary technique to deep inelastic neutron scattering (INS), the traditional technique used for this purpose [1,4]. This is not a trivial issue since Eq. (1) is based on the assumption that the electron dynamics is "instantaneous" compared to the atomic one, and that a relevant amount of electronic charge is present on the atom on a length scale smaller than $1/q$: these assumptions are decreasingly valid with increasing q . Specifically, we present in this Letter the results of a high resolution inelastic x-ray scattering experiment in liquid neon. We show that in the ± 100 meV exchanged energy range and for $q > 6 \text{ \AA}^{-1}$ the deep inelastic scattering regime is approached by the x rays scattered by the neon core electrons with effective mass equal to the atomic mass. We show, moreover, that IXS can be quantitatively used to determine atomic momentum distributions, as is demonstrated by the comparison between the present IXS results and those obtained by INS experiments [5–9]. Additionally, we show that the consistency between IXS and INS results is not limited to the determination of momentum distributions, but also holds for the more subtle determination of the final state effects in the scattering process.

The experiment was carried out at the beam line ID16 at the European Synchrotron Radiation Facility using the 2.6-m-long vertical spectrometer arm. The monochromatic x-ray beam at the sample position was characterized by an energy of ≈ 17.794 eV, a spot of $250 \times 80 \mu\text{m}^2$ horizontal \times vertical sizes, and an average flux of $\approx 5 \times 10^9$ photons/s. The q values investigated here are comprised between 1.0 and 16.0 \AA^{-1} , the latter value being achieved at scattering angles close to backscattering. At each q value an energy scan has been performed. The q resolution, defined by two slits placed in front of the analyzer, depends on q and is at most 3% of the corresponding q value. The energy resolution was q independent for $q > 2 \text{ \AA}^{-1}$ with a full width at half maximum of 6.9 meV.

The sample container was a 7.5 mm internal diameter 0.25-mm-thick Plexiglas tube. 99.99% pure natural neon gas was condensed directly into the container. The liquid neon sample was kept at a temperature of 27.6 ± 0.1 K and at a pressure of 1.4 ± 0.2 bar, corresponding to a density of ≈ 35.8 atoms/nm³ [10]. Empty container spectra were also recorded and subtracted to obtain the final spectra. Beside the lowest q spectrum at 1 \AA^{-1} , this subtraction is not critical since, in the adopted experimental setup, the empty container contribution amounts at most to a few percent of the total signal; in particular, for $q > 6.0 \text{ \AA}^{-1}$ the empty container spectra are indistinguishable from the flat electronic detector background of 0.4 counts/min.

The final spectral intensities at selected q values are reported in Fig. 1. They appear as a structureless peak which, with increasing q , shifts towards higher energies and becomes broader. Qualitatively, the observed q dependence is consistent with the INS results in the impulse approximation regime [5–9]: on approaching this regime, the dynamic structure factor is expected to shift in energy as q^2 and to broaden as q . In the IXS case at high q values, i.e., $q > 6 \text{ \AA}^{-1}$, the x rays are effectively scattered only by the core electrons, since the contribution of the outer electrons to the atomic form factor, $f(q)$, becomes negligible. In the scattering process, therefore, the core electrons acquire an effective mass which is given by the atomic mass, and through this channel the IXS spectrum reflects the *atomic* momentum distribution. Our aim is to account quantitatively for this picture. For this reason, we will use Eq. (1) to analyze our data, and we will then compare our results with those obtained in INS experiments [5–9], where a refined data analysis requires that both the

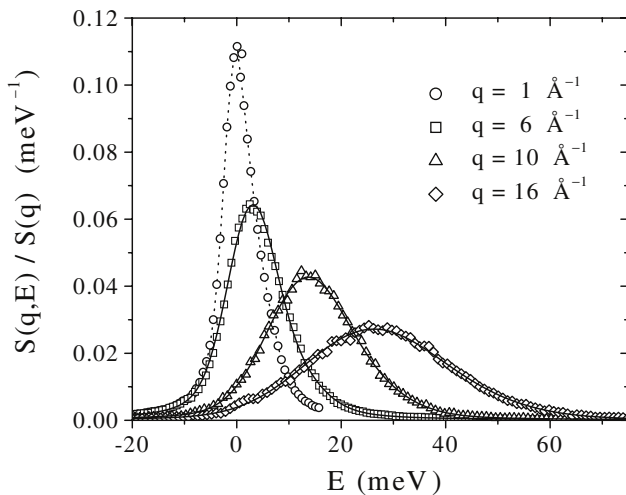


FIG. 1. Normalized spectral intensities of liquid neon at selected q values after subtraction of the empty container contribution. The typical accumulation time was ≈ 80 s/channel at $q < 10.0 \text{ \AA}^{-1}$, and about twice that at larger q values. The solid lines correspond to the results of the fit of Eq. (2) to the experimental data; the dashed line superimposed on the $q = 1 \text{ \AA}^{-1}$ spectrum is a guide to the eye.

actual shape of the momentum distribution and the final state effects have to be properly taken into account. These latter effects are due to the fact that the impulse approximation is reached only asymptotically: the struck atom cannot be considered to recoil completely freely from the collision, and the effects coming from its interaction with the neighboring atoms have to be taken into account. There are several ways of handling these final state effects [11]; we use here the so-called *additive approach* [12], which has already been shown to work well [8,9]. This approach amounts to expanding the intermediate scattering function in cumulants of powers of time, and then to retaining only the first few terms of such an expansion. If only the first three terms are retained, then the $S(q, E)$ can be approximated as [12]

$$S(q, E) \approx S_G(q, E) + S_1(q, E) + S_2(q, E), \quad (2)$$

where $S_G(q, E)$ is the dominant Gaussian contribution and $S_1(q, E)$ and $S_2(q, E)$ are the first two corrections to it. In more detail, these three terms read [12]

$$\begin{aligned} S_G(q, E) &= \frac{S(q)}{\sqrt{2\pi\mu_2}} \exp\left[-\frac{(E - E'_R)^2}{2\mu_2}\right], \\ S_1(q, E) &= -\frac{\mu_3}{8\mu_2^2} (E - E'_R) \left(1 - \frac{E'_d}{3}\right) S_G(q, E), \\ S_2(q, E) &= \frac{\mu_4}{8\mu_2^2} \left(1 - 2E'_d + \frac{E'_d}{3}\right) S_G(q, E). \end{aligned} \quad (3)$$

Here, $S(q)$ is the static structure factor; $E_R = \hbar^2 q^2 / (2M)$ is the recoil energy of the struck atom and M is its mass; $E'_R = E_R / S(q)$; μ_2 , μ_3 , and μ_4 are parameters related to the second, third, and fourth spectral moments of $S(q, E)$; $E'_d = (E - E'_R)^2 / \mu_2$. In particular, in the incoherent limit the parameters μ_2 , μ_3 and μ_4 have the following q dependence [4,12]:

$$\begin{aligned} \mu_2 &= \frac{\hbar^2 q^2}{M^2} \langle p_q^2 \rangle, \\ \mu_3 &= \frac{\hbar^4 q^2}{6M^2} \langle \nabla^2 V(r) \rangle, \\ \mu_4 &= \frac{\hbar^4 q^2}{M^2} \langle F_q^2 \rangle + \frac{\hbar^8 q^4}{M^4} \bar{\alpha}_4. \end{aligned} \quad (4)$$

Here, $\langle p_q^i \rangle$ is the i th moment of the momentum distribution function, $n(\mathbf{p})$, along \mathbf{q} ; $\bar{\alpha}_4 = \langle p_q^4 \rangle - 3\langle p_q^2 \rangle^2$; $V(r)$ is the pair potential energy; $\langle F_q^2 \rangle$ is the average square force in the direction of \mathbf{q} acting on the struck particle. Then, by fitting Eq. (2) to the experimental spectra at several q values and exploiting Eqs. (4), it is possible to obtain information on $n(\mathbf{p})$ and on the final state effects through the determination of $\langle \nabla^2 V(r) \rangle$ and of $\langle F_q^2 \rangle$.

We performed this analysis on the spectra measured at $q \geq 6 \text{ \AA}^{-1}$, where the incoherent approximation can be considered to be valid [9]. In the fitting procedure we left, besides an overall intensity coefficient, four free

parameters, namely, E_R , μ_2 , μ_3 , and μ_4 . The considered model can be adjusted very well to our experimental data, as shown in Fig. 1, and, in more detail, in the example reported in Fig. 2. The final χ^2 values are consistent with the number of the experimental points. In Fig. 2 we also report the separate contributions of the three terms of Eq. (2) to the $S(q, E)$. As Fig. 2 shows, the Gaussian term $S_G(q, E)$ describes most of the line shape, and consequently the parameters E_R (Fig. 3a) and μ_2 (Fig. 3b) are easily determined. The term $S_1(q, E)$ is very important in the fits since it accounts for the asymmetry of the experimental data, and therefore the parameter μ_3 (Fig. 3c) is also easily determined. The term $S_2(q, E)$ is conversely much less relevant: it can only be extracted from the low- q data, and even there the parameter μ_4 (Fig. 3d) is affected by a large uncertainty. In particular, for $q > 13 \text{ \AA}^{-1}$, the presence of this term is no longer statistically significant, and thus it has been neglected.

The theoretical expectations Eqs. (4) can be fitted to the values obtained for E_R , μ_2 , μ_3 , and μ_4 , and the results are shown in Fig. 3. In particular, E_R comes out with the expected q^2 dependence, from which it is possible to extract the value for the effective mass of the neon core electrons, $M = (19 \pm 3) \text{ u.m.a.}$, which is consistent with the neon atomic mass. This confirms that we are re-

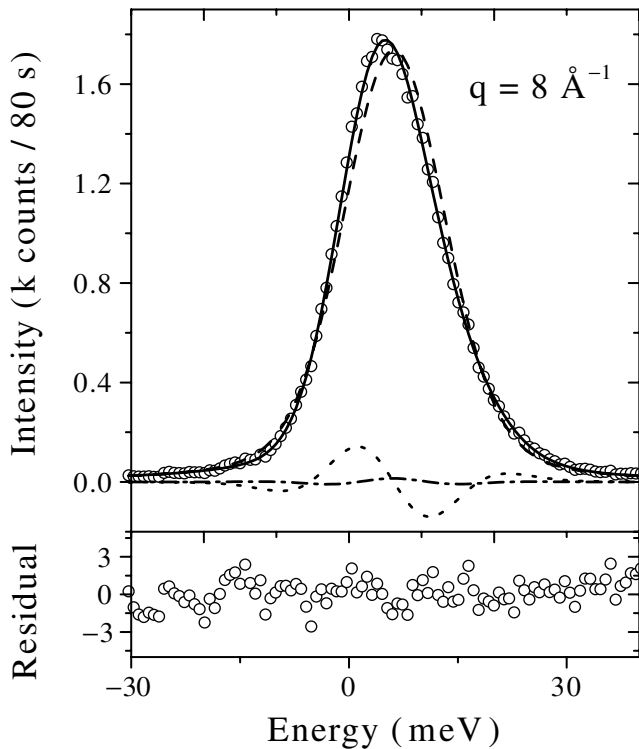


FIG. 2. Upper part: the spectrum of liquid neon at $q = 8 \text{ \AA}^{-1}$ is reported together with the best fit of Eq. (2) to the data (solid line). The individual contributions to Eq. (2) are also reported: $S_G(q, E)$ (dashed line), $S_1(q, E)$ (dotted line), and $S_2(q, E)$ (dot-dashed line). Bottom part: Residuals of the fit, in standard deviation units.

ally approaching the impulse approximation limit for atomic scattering. Moreover, also the μ_2 and μ_3 parameters show the expected q^2 dependence, and the values for the kinetic energy $\langle E_K \rangle = 3\langle p_q^2 \rangle / (2MK_B)$ and for $\langle \nabla^2 V(r) \rangle$ are readily extracted, see Table I. For what concerns μ_4/q^2 , conversely, there are too few and scattered points to significantly check its expected dependence; we then merely assume that $\hbar\alpha_4 = 0$ [13], and extract a value for $\langle F_q^2 \rangle$, see Table I. The values for $\langle E_K \rangle$, $\langle \nabla^2 V(r) \rangle$ and $\langle F_q^2 \rangle$ that are obtained here are compared in Table I with the experimental data available on liquid neon from INS experiments. The thermodynamic point which has been studied here is quite close to those studied in Refs. [5,7–9] and to one of those studied in Ref. [6]. It is possible to verify that the values that we obtain for $\langle E_K \rangle$, $\langle \nabla^2 V(r) \rangle$, and $\langle F_q^2 \rangle$ agree well, within the quoted error bars, with the available neutron scattering determinations [5–9]. An additional consistency check of the present analysis can be obtained from an expression of $\langle E_K \rangle$ worked out from a moment expansion of the momentum spectrum [5]:

$$\langle E_K \rangle = \frac{3T}{2} \left[1 + \frac{x^2}{12} - \frac{x^4}{240} + \frac{x^6}{2016} - \frac{x^8}{11520} + \frac{x^{10}}{253440} - \dots \right], \quad (5)$$

where $x^2 = \hbar^2 \langle \nabla^2 V(r) \rangle / (3MT^2)$. This expression connects $\langle E_K \rangle$ and $\langle \nabla^2 V(r) \rangle$. As a matter of fact, using the derived value for $\langle \nabla^2 V(r) \rangle$, we obtain $\langle E_K \rangle = (52 \pm 2) \text{ K}$, which is in very good agreement with the value extracted from the q dependence of μ_2 .

In conclusion, we have reported an experimental study of the inelastic scattering of x-rays from liquid neon in the $\pm 100 \text{ meV}$ exchanged energy range and in the q range between 1 and 16 \AA^{-1} . We have shown that the measured spectra can be consistently analyzed within the impulse

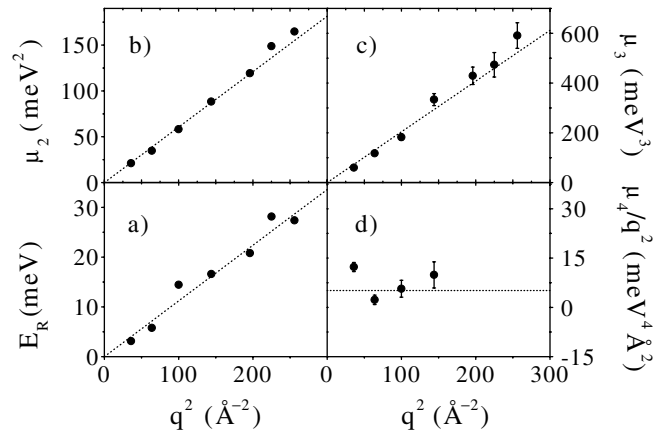


FIG. 3. The results (circles) for the relevant parameters obtained by fitting Eq. (2) to the measured IXS spectra: E_R (a), μ_2 (b), μ_3 (c), and μ_4 (d). The theoretical expectations, Eqs. (4), can be well adjusted to the obtained results, and are reported as dashed lines.

TABLE I. Comparison between the present IXS results and the results obtained on neon in neutron scattering experiments. The data for ρ have been derived from Ref. [11] when missing in the original papers. The value for $\langle \nabla^2 V(r) \rangle$ attributed to Ref. [8] has been worked out from the A_3 coefficients tabulated there.

T [K]	ρ [atoms/nm ³]	$\langle E_k \rangle$ [K]	$\langle \nabla^2 V(r) \rangle$ meV Å ⁻²	$\langle F_q^2 \rangle$ meV ² Å ⁻²	Refs.
26.9	36.3	48.2 ± 0.9	—	—	[5]
25.8	36.3	52.8 ± 3.7	—	—	[6]
35.1	34.6	69.0 ± 4.7	—	—	[6]
35.3	31.7	66.4 ± 3.3	—	—	[6]
27	35.8	—	280 ± 70	—	[7]
25.8	36.7	52.5 ± 2.1	350 ± 40	280 ± 70	[8]
25.8	36.7	52.9 ± 2.5	372 ± 43	200 ± 200	[9]
27.6	35.8	51 ± 3	280 ± 40	170 ± 100	This work

approximation if we additionally take into account the final state effects, and the results we obtain from this analysis are consistent with those derived from INS experiments [5–9]. This demonstrates that inelastic x-ray scattering can be effectively used to obtain quantitative information on *atomic* momentum distributions in condensed matter, thus providing a complementary technique to deep inelastic neutron scattering.

This complementarity could be particularly useful for the study of the atomic momentum distribution in polyatomic or polyisotopic systems, where switching from INS to IXS could allow one to change the relative contrast of the atomic/isotopic species present in the system, and the x-ray probe would effectively correspond to an additional available isotopic substitution. Actually, there are several open problems where the joint use of INS and IXS could come out to be particularly interesting. One example could be the study of ³He, a case of broad interest but irksome for neutron scattering due to its large absorption; or, more in general, the study of ³He-⁴He mixtures, where the results of INS experiments and those of the most recent microscopic calculations still show important discrepancies [14]. Another interesting example could be the study of hydrogen, the reference case for INS, where interesting anomalies in the neutron scattering cross section have been recently observed [15]. Similarly, the use of IXS can also be useful in the study of hydrogen isotope mixtures, which are made difficult for INS because of the huge difference of cross sections among the various hydrogen isotopes.

We acknowledge Professor W.G. Stirling for pointing us to the case of liquid neon, and C. Henriquet for his technical assistance.

- [1] An overview of these experiments can be found in *Momentum Distributions*, edited by R. N. Silver and P. Sokol (Plenum, New York, 1989).
- [2] W. Schulke, in *Handbook on Synchrotron Radiation*, edited by G. Brown and D. Moncton (Elsevier, New York, 1991), Vol. 3, pp. 565–637.
- [3] W. M. DuMond, Phys. Rev. **33**, 643 (1929).
- [4] V. F. Sears, Phys. Rev. B **30**, 44 (1984).
- [5] V. F. Sears, Can. J. Phys. **63**, 68 (1985).
- [6] D. A. Peek, M. C. Schmidt, I. Fujita, and R. O. Simmons, Phys. Rev. B **45**, 9671 (1992).
- [7] M. A. Fradkin, S.-X. Zeng, and R. O. Simmons, Phys. Rev. B **49**, 15 563 (1994).
- [8] R. T. Azuah, W. G. Stirling, H. R. Glyde, P. E. Sokol, and S. M. Bennington, Phys. Rev. B **51**, 605 (1995).
- [9] R. T. Azuah, W. G. Stirling, H. R. Glyde, and M. Boninsegni, J. Low Temp. Phys. **109**, 287 (1997).
- [10] C. Gladun, Cryogenics **6**, 27 (1966); *ibid.* **7**, 78 (1967).
- [11] A discussion of several treatments of the final state effects can be found in T. R. Sosnick, W. M. Snow, R. N. Silver, and P. E. Sokol, Phys. Rev. B **43**, 216 (1991).
- [12] H. R. Glyde, Phys. Rev. B **50**, 6726 (1994).
- [13] This assumption is essentially compatible with the INS results reported in Refs. [8,9], where it is shown that the parameter $\hbar\alpha_4$ is indeed very small. This means that the momentum distribution of liquid neon is practically Gaussian.
- [14] M. Boninsegni and S. Moroni, Phys. Rev. Lett. **78**, 1727 (1997); R. T. Azuah, W. G. Stirling, J. Mayers, I. F. Bailey, and P. E. Sokol, Phys. Rev. B **51**, 6780 (1995).
- [15] C. A. Chatzidimitriou-Dreismann, T. Abdul Redah, R. M. F. Streffer, and J. Mayers, Phys. Rev. Lett. **79**, 2839 (1997); E. B. Karlsson and S. W. Lovesey, Phys. Rev. A **61**, 062714 (2000).